

Detecting Popular Temporal Modes in Population-scale Unlabelled Trajectory Data

FENGLI XU, TONG XIA, HANCHENG CAO, and YONG LI, Tsinghua University
FUNING SUN and FANCHAO MENG, Tencent Inc.

With the rapid process of urbanization, revealing the underlying mechanisms behind urban mobility has become a crucial research problem. The movements of urban dwellers are often constituted by their daily routines, and exhibit distinct and contextual temporal modes, i.e., the patterns of individuals allocating their time across different locations. In this paper, we investigate a novel problem of detecting popular temporal modes in population-scale unlabelled trajectory data. Our key finding is that the detected temporal modes capture the semantic feature of human's living style, and is able to unravel meaningful correlations between urban mobility and human behavior patterns.

Specifically, we represent the temporal mode of a trajectory as a *partition* of the time duration, where the time slices associated with same locations are partitioned into same subsets. Such abstraction decouples the temporal modes from actual physical locations, and allows individuals with similar temporal modes yet completely different physical locations to have similar representations. Based on this insight, we propose a pipeline system composed of three components: 1) noise handler that eliminates the noises in the raw mobility records, 2) representation extractor for temporal modes, and 3) popular temporal modes detector. By applying our system on three real-world mobility data sets, we demonstrate that our system effectively detects the popular temporal modes embedded in population-scale mobility data sets, which is easy to be interpreted and can be justified through the associated PoIs and mobile applications usage. More importantly, our further experiments reveal insightful correlations between the popular temporal modes and individuals' social economic status, i.e. occupation information, which sheds light on the mechanisms behind urban mobility.

CCS Concepts: • Information systems → Data mining; • Human-centered computing → *Empirical studies in ubiquitous and mobile computing*;

Additional Key Words and Phrases: temporal modes, mobility data, human behaviour modelling.

ACM Reference format:

Fengli Xu, Tong Xia, Hancheng Cao, Yong Li, Funing Sun, and Fanchao Meng. 2017. Detecting Popular Temporal Modes in Population-scale Unlabelled Trajectory Data. *Proc. ACM Interact. Mob. Wearable Ubiquitous Technol.* 0, 0, Article 0 (2017), 27 pages.

DOI: 0000001.00000001

1 INTRODUCTION

The daily movements of urban dwellers are often driven by social and economic purpose, and consist of regular transitions and visits between contextual locations, such as commuting between homes and offices. Therefore, the temporal modes, i.e., the regular patterns of individuals allocating their time on different

This work is supported by XXXXXX.

Permission to make digital or hard copies of all or part of this work for personal or classroom use is granted without fee provided that copies are not made or distributed for profit or commercial advantage and that copies bear this notice and the full citation on the first page. Copyrights for components of this work owned by others than ACM must be honored. Abstracting with credit is permitted. To copy otherwise, or republish, to post on servers or to redistribute to lists, requires prior specific permission and/or a fee. Request permissions from permissions@acm.org.

© 2017 ACM. 2474-9567/2017/0-ART0 \$15.00

DOI: 0000001.00000001

contextual locations, form the blueprint of urban mobility and are deeply embedded in their trajectories. For example, a government employee may spend a typical working day among the visit and transition between office and home, while a salesman may allocate the typical working day among multiple different locations for business meetings. Detecting and understanding the popular temporal modes among large scale population sheds light on the mechanism behind human mobility, which will significantly benefits a wide range of applications, such as user profiling, mobile advertisement, and business intelligence[1, 2].

Thanks to the ever-increasing penetration rate of mobile devices, massive amount of fine-grained mobility data has been ubiquitously sensed and collection. Although substantial solutions have been proposed to model and understand the patterns of human behaviours [3, 4], they fell short of detecting popular temporal modes embedded in mobility data in two aspects. 1) *Similarity metric*: Many previous works in trajectory mining aimed to detect the popular mobility patterns by identifying the clusters of trajectories that share similar sub-trajectories or co-occurrence with high frequency [4, 5]. As a result, these approaches could not measure the contextual similarities in temporal mode, and hence failed to recognize the popular temporal modes embedded in mobility data. 2) *Human-labeled data*: Substantial works on modelling and understanding the patterns of human behaviors relies on human-labeled behavior logs[3], which prevents them to scale for detecting the popular temporal modes in large scale. Different from previous works, in this paper we aim to address the research problem of efficiently and effectively detecting the contextual temporal modes embedded in population-scale unlabelled mobility data.

Despite of its great importance, detecting the popular temporal modes embedded in the trajectories of a large population is non-trivial. The key challenge is devising an appropriate representation to capture the feature of temporal modes in mobility data. The representation should meet following two requirements: 1) the representations should be suitable for measuring the similarities in temporal mode, which indicates that the trajectories with similar temporal modes should have similar representation; 2) preserving the contextual information of temporal modes, which implies that the representation should have clear physical meaning and easy to interpreted.

To fulfill these requirements, we leverage two key insights to devise the representation: firstly, although the same locations may mean different contexts for different individuals, they usually implicate similar contexts for one individual; secondly, the temporal modes can be characterized as the patterns of individuals allocating their time on different contextual locations. Specifically, we first segment the time period into a series of time slices, and then we represent the temporal mode of an individual as a partition of the set of time slices, where the time slices associated with the same location are partitioned into same subsets. For example, the typical nine to five working schedule may result in a partition with 9:00AM~5:00PM in a subset and 5:00PM~9:00AM in another subset. Such abstraction decouples individual's temporal modes from physical locations, and allows the individuals with similar temporal modes yet having large spatial distance to own similar representations. Based on this representation extraction method, we propose a pipeline system to identify the popular temporal modes in three steps: 1) firstly, we introduce a density based clustering technique to handle the noises in raw mobility data by identifying the mobility records with slightly different spatial coordinates but actually corresponding to the same venues; 2) secondly, we extract the representation of temporal modes from each individual's denoised mobility records; 3) finally, we introduce a distance metric to properly measure the similarities between the representations, and devise an unsupervised clustering algorithm to automatically detect the popular temporal modes by finding the major clusters.

To evaluate the performance of our system, we utilize three large scale real-world mobility data sets collected from mobile application, cellular network and travel survey. By applying our system on these three data sets, we make following interesting observations. First of all, our system successfully detects distinct popular temporal modes for each data set. The identified popular temporal modes are easy to

be interpreted and consistent with the common intuitions of urban dwellers' daily lives, such as regular working schedule and hanging out in the weekend. Secondly, by leveraging the points of interest and mobile applications usages associated with the mobility records, we conduct rigorous hypothesis testing on whether the mobile users with different temporal modes deviate their behaviors from the general population. The results reveal that mobile users of different temporal modes do have meaningful and significantly different features in their daily behaviours, which justifies the identified temporal modes and brings semantics to them. For example, the users with regular working schedules have significantly higher possibility in visiting company and government area during working hours. **Last but not least, through analyzing the self-reported occupation information in mobile application and travel survey datasets, we unravel insightful correlations between individual's temporal mode and social economic status.** For example, the individuals with nine to five working schedule are more likely have occupations in professional, managerial and technical category, while individuals with earlier working schedule are more likely to have occupations in manufacturing, constructing and farming category. By leveraging these correlations, our system achieves significant performance gains comparing with the baseline algorithm in both classifying trajectories into occupations and mobility records into PoI visitations.

The rest of this paper is organized as follows. We systematically review the related works in Section 2, and discuss the motivations and key challenges of our work in Section 3. Motivated by the challenges, we design a pipeline system that can effectively and efficiently identify the popular temporal modes in Section 4. After that, we apply our system on three real-world mobility data and conduct extensive analysis on the derived temporal modes in Section 5. We discuss the limitations and future works in Section 6, and finally conclude our paper in Section 7.

2 RELATED WORK

The past decade has witnessed a dramatic proliferation of mobility data set, which provides a reliable medium for detecting and understanding the daily behavior of mobile users. Now, we summarize the related works from three perspectives.

Trajectory clustering: Extensive researches have been dedicated to identifying similar trajectory clusters in large scale mobility data[4, 6]. Lee et al.[4] proposed a *partition-and-group* framework to group trajectories based on the over-lapping sub-trajectories shared by them. [5] and [7] devised algorithms to first extracted latent mobility features with principal component analysis, and then clustered trajectories in the latent space. These previous works mostly identified trajectory clusters by measuring the co-occurrence of spatiotemporal points, which usually led to grouping physically nearby trajectories and cannot preserve semantics. As for semantic trajectory clustering, Ying[6] proposed *semantic-trajectory-similarity* metric to measure the similarity of trajectories based on the associated PoIs. However, this approach labeled the semantic of spatiotemporal points as the type of associated PoIs, which is invalid since same types of PoI can mean different semantics for different people. In this paper, we investigate a novel problem of clustering trajectories based on their temporal modes, which is a valid and flexible semantic similarity metrics for trajectories.

Mobility patterns modeling: The proliferation of mobility data facilitates a bunch of researches in mobility pattern modeling. As for frequent mobility routines, Giannotti et al. [8] proposed *T-patterns* to address the problem of efficiently mining frequent spatiotemporal point sequences. Mamoulis et al. [9] studied the problem of mining frequent periodic mobility patterns, while Zheng et al. [10] aimed to detect the frequent traveling path between fixed locations. In addition, several previous works studied the patterns of mobility data's generative process. Becker et al. [11] utilized call detail record to investigate the generating of home-to-work carbon footprints. Isaacman et al. [12] proposed *WHERE* to model the mobility patterns and synthetic mobility records, while Jiang et al. [13] designed *timegeo* framework to

model urban mobility and generate fine-grained mobility traces without travel survey. Different from previous works, in this paper we aim to model the temporal modes of population-scale trajectory data, which is the pattern of allocating time across different locations.

Urban activity recognition: With the rapid process of urbanization, many researchers have been drawn to study the problem of modeling urban activity. In urban geographic topic discovery, [14] and [15] extended the topic model to discover the semantic context of urban area with mobility data and social media check-ins, respectively. [16] and [17] analyzed the cellular traffic consumption patterns and mobility patterns in urban area, and linked them with function of urban area. As for the urban dynamics, Cranshaw[18] exploited the social media check-ins in foursquare to urban area into dynamic communities based on spatial distance as well as social proximity; Daggitt et al. [19] modeled the dynamic of urban activity with the PoI data in location-based service; Zhang et al.[20] proposed a cross-modal embedding algorithm to model the dynamics of urban activities with geo-tagged social media data. These works modeled the semantic context of urban area in static and homogenous manner [14–16, 18, 20]. In contrast, we devise an appropriate representation that can map the same urban area to different semantics for different individuals or at different time, which achieves valid feature extractions.

3 MOTIVATION AND CHALLENGES

The daily movements of modern urban dwellers often exhibit regular temporal modes, such as nine to five working schedule, hanging out in park during weekend morning, and so on. Previous work has demonstrated that individual's mobility is theoretically highly predictable due to its regularity[21]. Therefore, detecting the popular temporal modes shared by large population sheds light on the blueprint of urban mobility, which is able to facilitate a wide range of applications in public administration, business intelligence and disease controlling. More importantly, individual's temporal mode is usually correlated with their social economic status. For example, a government employee usually leads a temporal mode corresponding to nine to five working schedule during working day, while boarding school students usually stay in one location. Therefore, detecting and understanding the popular temporal modes is able to help us infer the social economic status of individuals and achieve more accurate user profiling.

Despite of its importance, detecting popular temporal modes in large scale unlabelled mobility data also poses significant challenges, which the previous trajectory mining algorithms fell short to address. In this paper we aim to tackle this problem by designing a three step pipeline system, which is motivated by the following three major challenges.

Extracting representations for temporal modes: Achieving a suitable and context preserving representations for temporal modes is challenging for two reasons. Firstly, the representations should be suitable for measuring the similarities in temporal modes. The physically nearby trajectories are likely to share similar spatiotemporal points, while the trajectories are similar in temporal modes yet remote in distance are not, which might cause biases in the similarity metric. Hence, the representations should be able to decouple the temporal mode from actual physical locations. Secondly, the passively collected mobility records are usually large scale yet unlabelled, which means we do not know the context behind users' mobility records. In order to preserve the context in temporal modes, we need to derive a representation that is able to context information. However, without any supervised information it is hard to infer the context of each mobility records. To make matters worse, the same locations could mean different context for different users. For example, a restaurant is place for food for customers, while it is a working place for chefs. Therefore, the context of each mobility record cannot be solely determined by its location.

Handling noises in raw mobility records: Mobile users generate massive amount of mobility records through their mobile devices with either GPS modules or network-based localization services.

These raw records are often with noises and errors due to the inaccuracy of localization[22]. Such noises pose serious challenge for detecting the temporal modes embedded in them. On one hand, it is hard to infer the context information, such as staying in home or working in office, from noisy mobility records, because even staying in the same location mobile users could generate mobility records with different spatial locations. On the other hand, the noises also cause the problem of data sparsity, because almost all the mobility records are with different spatial coordinates. Therefore, detecting the temporal modes in noisy mobility data is challenging, and a carefully designed context preserving de-noise scheme is needed.

Identifying popular temporal modes: Even with the extracted representation for temporal modes, identifying popular temporal modes is still non-trivial in terms of two aspects. 1) Without any prior information about the potential popular temporal modes, we need to design an unsupervised scheme to effectively and efficiently detect the popular temporal modes, which should be able to handle heterogenous behaviors of different users as well as large scale mobility records. 2) Since different mobile users' temporal modes are unlikely to be identical, we need to design a similarity metric properly measures the closeness between different temporal modes, which is difficult because the representation of different temporal modes is heterogenous. For example, different users could have significantly different number of contextual locations.

4 METHOD

We aim to design a methodology that is able to detect the popular temporal modes embedded in population-scale unlabelled mobility data. To achieve this goal, we are dedicated to answering two questions: 1) how to extract suitable representations for temporal modes? and 2) how to detect popular temporal modes without any prior knowledge? In this section, we design a pipeline system that can effectively and efficiently addresses the identified challenges. We first give a concise overview of our system, and then elaborately describe the design of each component in our system.

4.1 Overview

Motivated by the identified key challenges, we break down the problem of detecting popular temporal modes into three sub-problems: 1) handling the noise in raw mobility records; 2) extracting good representations for temporal modes; 3) detecting popular temporal modes. We design a pipeline system that addresses these sub-problems one by one, which is illustrated in Figure 1. It is composed of three components: noise handler, representations extractor and popular temporal modes detector, which respectively solves the above three problems.

Firstly, the noise handler takes in raw mobility records as input and de-noises them by identifying the records that are actually created in same venues yet have slightly different location coordinates. To achieve this goal, we propose a density based clustering algorithm to automatically detect the venues behind the noisy mobility records, which are presented in the left part of Figure 1. It effectively addresses the problem of inaccurate localization as well as the sparsity of mobility records. After that, we design a representation extractor to derive contextual representations for temporal modes from the de-noised mobility records. The key idea is to represent the temporal modes as a *partition* of time slices, where the time slices associated with same locations are allocated to same subsets. The extracted representations are illustrated in Figure 1(c), where the time slices with different colors corresponding to different locations. Such extraction decouples the representations from actual physical locations while preserves the patterns of allocating time on different locations, which is crucial for identifying similar temporal modes. Finally, we propose a popular temporal modes detector to efficiently and effectively detect the popular temporal modes hidden in the representations of large scale population. Specifically, we introduce a distance metric

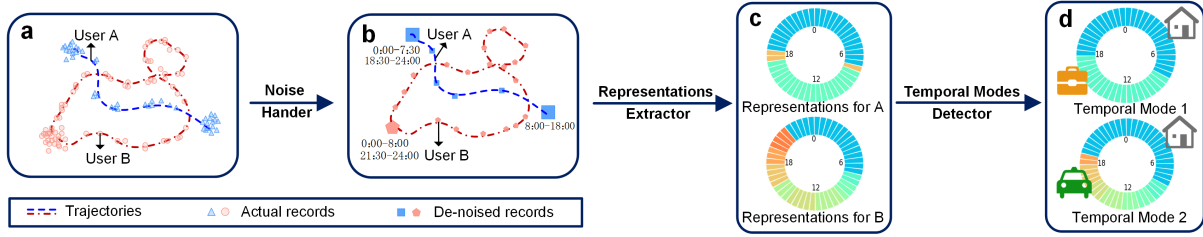


Fig. 1. Illustration of the proposed system for popular temporal modes detecting.

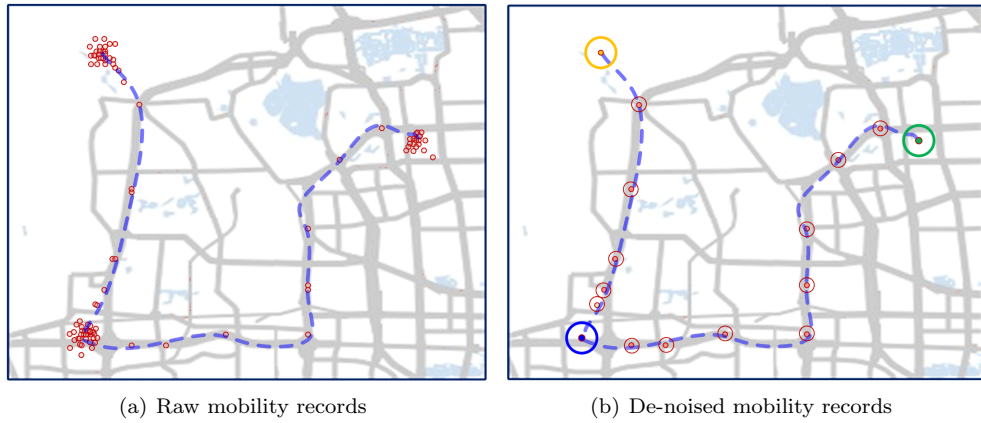


Fig. 2. De-noising the raw mobility records with density based clustering technique.

to properly measure the similarities between the representations, and detect the popular temporal modes by finding the major clusters with an unsupervised clustering algorithm.

4.2 Handling Noise via Density Based Clustering Algorithm

We first formally introduce the utilized denotations as follows. Denote D as the trajectory dataset and $T^i \in D$ as the trajectory of the i -th individual in the dataset. We denote its trajectory as $T^i = [r_1^i, r_2^i, \dots, r_m^i, \dots]$, where r_m^i is the m -th mobility record of the i -th individual. It can be expressed as a tuple $r_m^i = (l_m^i, t_m^i)$, with l_m^i and t_m^i denoting the location coordinate and time stamp, respectively. We denote the de-noised trajectory as $\hat{T}^i = [\hat{r}_1^i, \hat{r}_2^i, \dots, \hat{r}_m^i, \dots]$, where $\hat{r}_m^i = (\hat{l}_m^i, t_m^i)$ and \hat{l}_m^i is the location coordinate after the process of noise handling.

Figure 2(a) visualizes the spatial distribution of raw mobility records left by an individual. We can observe that although some of the records are likely to be created in the same venues, they have slightly different spatial coordinates due to the inaccuracy of localization and the spatial coverage of the venues. The goal of noise handler is to identify the mobility records corresponding to same venues, and replace their spatial coordinates with corrected coordinates, which is illustrated in Figure 2(b). **We address this problem by exploiting one key insight: for a certain venue, the spatial coordinates of associated mobility records distribute randomly around the actual location.** Therefore, the density peak of mobility records is close to actual location. Specifically, we define the density of a mobility record as the number of mobility

ALGORITHM 1: Localization Noise Handler via Density Based Clustering Algorithm.

Input: raw trajectory $T^i = [r_1^i, r_2^i, \dots, r_m^i, \dots]$, $r_m^i = (l_m^i, t_m^i)$; density kernel range d_c ; threshold θ .

Output: denoised trajectory \hat{T}^i .

Procedure:

```

distance matrix:  $\{d_{m,n} = dist(r_m^i, r_n^i) \mid \text{for } \forall r_m^i, r_n^i \in T^i\}$ 
for  $r_m^i \in T^i$  do
|    $\rho_m = \sum_n \xi(d_{m,n} - d_c)$  // step function:  $\xi(x) = 1$ , if  $x > 0$ ;  $\xi(x) = 0$ , otherwise.
|   end
for  $r_m^i \in T^i$  do
|    $\delta_m = \min_{n: \rho_n > \rho_m} (d_{i,j})$ ,  $\lambda_m = \arg \min_{n: \rho_n > \rho_m} (d_{i,j})$ 
|   end
 $V = [r_m^i \mid \text{for } \forall \delta_m > \theta]$ ,  $\hat{T}^i = [r_m^i \mid \text{for } \forall \delta_m > \theta]$  // List of identified venues;
for  $r_m^i \in T^i$  and  $r_m^i \notin V$  do
|    $p = m$ 
|   while  $r_p^i \notin V$  do
|   |    $p = \lambda_p$ 
|   |   end
|   |    $\hat{T}^i.append((l_p^i, t_m^i))$ 
|   end

```

records within a certain range from it, and the actual coordinates of venues are estimated by the mobility records with local maxima density. Motivated by this insight, we propose a density based clustering algorithm to handle the noise and locating errors[23]. The procedure of the denoising scheme is formally formulated in Algorithm 1. Specifically, given the raw mobility records of a mobile user, we compute two values for each mobility records: density ρ_m and shortest distance to a mobility records with higher density δ_m , where density is defined as number of mobility records within a predefined range d_c . Then, the spatial coordinates of mobility records with δ_m higher than a predefined threshold θ are identified as coordinates of distinct venues, which means that coordinates are local maxima of density within range of θ . Finally, we change the spatial coordinates of raw mobility records to the coordinates of nearest identified venues. It worth noting that the complexity of algorithm is $O(M^2)$ for a trajectory with M mobility records. To speed up and make it applicable to large scale mobility data, we first segment the space into 10 meters tiny grids and merge the mobility records within same grids. This effectively reduce the number of mobility records M by merging the records that are most likely of same venues, which significantly speeds up the denoising process and made it practical in large-scale mobility dataset.

4.3 Extracting Representation via Time Partition

The goal of representation extractor is to derive a proper representation that captures contextual temporal modes of the users from their mobility records. The extracted representation should meet the following requirements: 1) preserving the contextual information of temporal modes; 2) the similarities between representations should only depend on the temporal modes themselves, which implicates that mobile users with similar temporal modes yet large physical distance should have similar representation.

Deriving a representation that extracts contextual information from mobile user's movements is non-trivial. The key challenge is that different users may have different purposes for the same locations. To address this problem, we leverage a key insight that although the same location may implicate different

contexts for different users, it usually means similar context for the same user. Therefore, for each user, the time periods associated with same locations implicate similar context for her. Inspired by this insight, we characterize the temporal mode of mobile users as how they allocates their time on different contextual locations. Specifically, we discrete the movements of mobile users by segmenting the time duration into time slices and associate each time slice with the most frequent locations she visits in that time slice. **To capture the regular temporal modes and make different users' representations comparable, we first extract individuals' typical movement in working day and non-working day, and then represent the temporal modes of individuals as how they allocate their time in typical working and non-working day.** Formally, we denote the discrete regular movement of mobile user i as $\mu^i = [\kappa_1^i, \kappa_2^i, \dots, \kappa_U^i]$, where U is the total number of time slices. Then, denote $C = [\tau_1, \tau_2, \dots, \tau_U]$ as the collection of all the time slices, and define temporal mode P^i of mobile user i as the *partition* of C based on her discrete movement μ^i . The definition of P^i is as follows.

Definition 1 (Representation for temporal mode P^i): Given a collection of time slices $C = [\tau_1, \tau_2, \dots, \tau_U]$ and regular movement $\mu^i = [\kappa_1^i, \kappa_2^i, \dots, \kappa_U^i]$. A *partition* of C is a set of mutually exclusive non-empty subsets whose union is C . Let $V^i = [v_1^i, v_2^i, \dots, v_H^i]$ be the distinct venues in μ^i , temporal mode P^i is a *partition* of C , where:

$$P^i = \{S_1^i, S_2^i, \dots, S_H^i\}, \quad S_h^i = \{\tau_j \mid \forall \kappa_j^i = v_h^i\};$$

Specifically, we represent the temporal mode of each mobile user as a *partition* of the collection of time duration, where the time slices associated with same locations are assigned to same subsets. Figure 3 shows the basic idea and procedure of how to derive representations from the denoised trajectories. We first transform the trajectories into discrete transitions between different locations, and then express the representations as the way mobile users allocate their time on different locations. The time slices with same colors are time slices corresponding to same locations and are assigned to the same subsets accordingly. Such abstraction allows the same locations to be mapped to different contexts for different users, and captures the patterns of mobile users allocating their time on different contextual locations. More importantly, it decouples the actual physical locations from the representations, which enables extracting similar representations for mobile users that have similar time allocations yet completely different physical locations. As showing in Figure 3, users A and B have completely different trajectories and move in completely different spatial locations. However, since they have the same way of allocating time on different locations, which represents the same life style, we obtain the same representations for them under our proposed method. This procedure, which decouples the closed correlated temporal and spatial information in the trajectories, is crucial to identify popular temporal modes embedded in large scale unlabelled mobility data.

4.4 Detecting Popular Temporal Modes via Unsupervised Clustering

With the extracted representations for temporal modes, the remaining problem is how to detect the popular temporal modes hidden in large scale representations of large population. The key challenge is that we do not any prior knowledge about the popular temporal modes. Therefore, we need to propose a distance to measure the similarity between the representations and design an unsupervised method to cluster them. To achieve this goal, we first introduce a *distance metric* that can properly measure the similarity between representations, and then design an unsupervised algorithm to effectively identify the popular temporal modes.

4.4.1 Measuring the similarity between representations. Since we design the representation as a *partition* of the collection of time slices, we introduce the *partition distance*[24] as the similarity metrics between different representations. Formally, the *partition distance* is defined as follows.

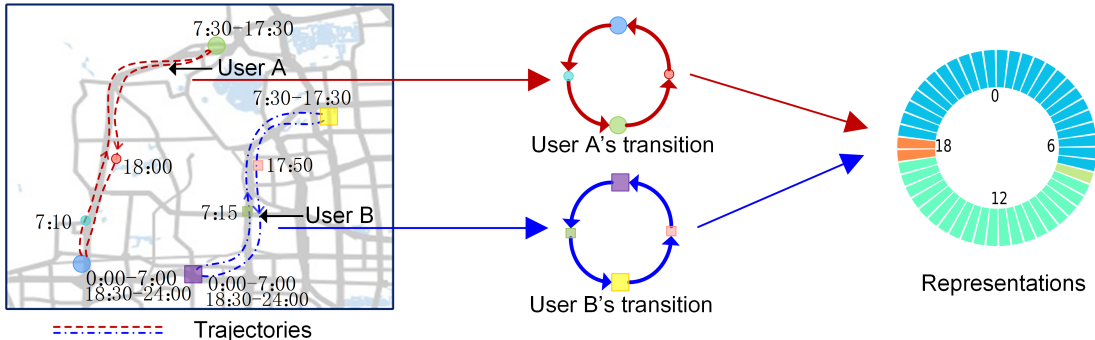
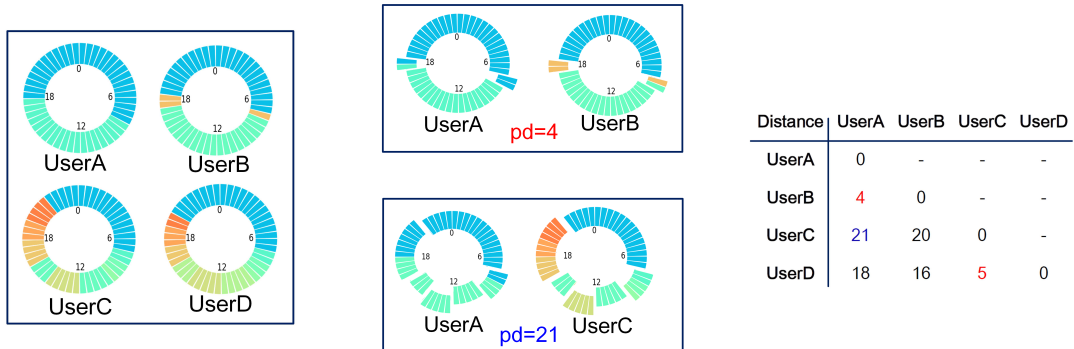


Fig. 3. Visualization of extracting representations from mobility records for temporal modes.



(a) Representations of 4 mobile users. (b) Measuring partition distance. (c) The summary of obtained distance.

Fig. 4. Visualization of measuring similarities between representations with partition distance.

Definition 2 (Partition Distance $pd(\star, \star)$): Given two partitions P^m and P^n of a collection of time slices C , the *partition distance* between P^m and P^n , $pd(P^m, P^n)$, is the minimum number of time slices that must be removed from C , so that the two induced partitions are identical.

It can be easily prove that *partition distance* is a proper *distance metric*, which possesses the nice properties of non-negativity, symmetry, identity of indiscernibles and triangle inequality[25]. Figure 4 visualizes the procedure of measuring *partition distance* between the representations of 4 mobile users. We can observe that the *partition distance* is able to properly measure the similarities between representations for temporal modes, where the similar temporal modes, e.g., user *A* and user *B*, have a small distance, while the different temporal modes, e.g., user *A* and user *C*, have a larger distance. It worth noting that the problem of computing *partition distance* has been proved to be equivalent to *Linear Assignment Problem*, and therefore it can be efficiently solved with *Hungarian Algorithm* in polynomial time[26, 27].

4.4.2 Identifying the popular temporal modes. To address the problem of no labeled mobility data, we proposed an unsupervised clustering method by exploiting the insight that the popular temporal modes

ALGORITHM 2: Popular Temporal Modes Detector via Unsupervised Clustering.

Input: collection of representations for temporal modes $\Gamma = [P^1, P^2, \dots, P^N]$, number of popular temporal modes k .

Output: collection of popular temporal modes $\Pi = [\pi_1, \pi_2, \dots, \pi_k]$.

Initialization: Π = randomly selected k representations from γ ; cluster assignments: $\Omega = [\omega_1, \omega_2, \dots, \omega_N]$.

Procedure:

```

stop = false.
while stop == false do
    |  $\omega_i = \arg \min_{j: \pi_j \in \Pi} (pd(P^i, \pi_j))$ , for  $\forall P^i \in \Gamma$ .
    |  $\Pi' = \Pi$ .
    | for  $j = 1$  to  $k$  do
        |   |  $\pi_j = \arg \min_{P^i: \omega_i=j} (\sum_{\omega_h=j} pd(P^i, P^h))$ .
        | end
        | if  $\Pi' == \Pi$  then
        |   | stop = true.
        | end
    end
end

```

should be shared by a group of mobile users. Therefore, the representations for popular temporal modes should be close to many individuals' representations, which implicates that they are the centers in the clusters of similar representations. Hence, we leverage the idea of *partition around medoids* in clustering analysis to automatically discover the clusters of temporal modes by measuring the similarities between them[28]. The proposed algorithm of detecting popular temporal modes is presented in Algorithm 2. Specifically, we first randomly select k representations as the medoids of clusters. Then, we iteratively assign the representations to the nearest medoid to form clusters, and update the medoids as the representations that have minimum sum of distance to other representations in the cluster, until the medoids are stable. Finally, the temporal mode represented by medoid of detected cluster is identified as the popular temporal mode adopted by the mobile users within that cluster. The clustering method is a variant of k-means algorithm. Different from k-means, it uses the medioids point instead of arithmetic mean as the center of each cluster. The underlying design rationale is that the temporal modes are represented as the partitions of time slices, which prohibits the operation of deriving arithmetic mean. As for the parameter setting, we iteratively search the number of popular temporal mode k at different value with empirical experiments, and finally fix k as the largest value that produce stable and distinctive popular temporal modes. The proposed algorithm detects the popular temporal modes solely based on the similarities between the representations of temporal modes. Therefore, it is unsupervised and effectively addresses the problem of no labeled mobility data.

To conclude, we propose a pipeline system to address the problem of detecting popular temporal modes in population-scale unlabelled mobility records. There are three components in the pipeline system: 1) a noises handler which leverages density-based clustering algorithm to identify the mobility records corresponding to same venues; 2) a representation extractor that decouples the physical locations from the temporal mode, and represents the temporal mode as a *partition* of time slices; 3) a popular temporal modes detector which exploits an unsupervised clustering algorithm to automatically detect the popular temporal modes as the medoids of major clusters.

Sources \ Features	Origin	Localization Method	Duration	Number of Users	Users with Occupations
Mobile applications	Beijing, China	GPS module	17 Sep.~31 Oct. (2016)	100,000	103
Cellular network	Shanghai, China	Cellular base station	1 Apr.~7 Apr. (2016)	100,000	0
Travel survey[29]	USA	Self-reported location	Mar. (2008)~ Mar.(2009)	11,712	11712

Table 1. Key features of three real world mobility datasets we utilize.

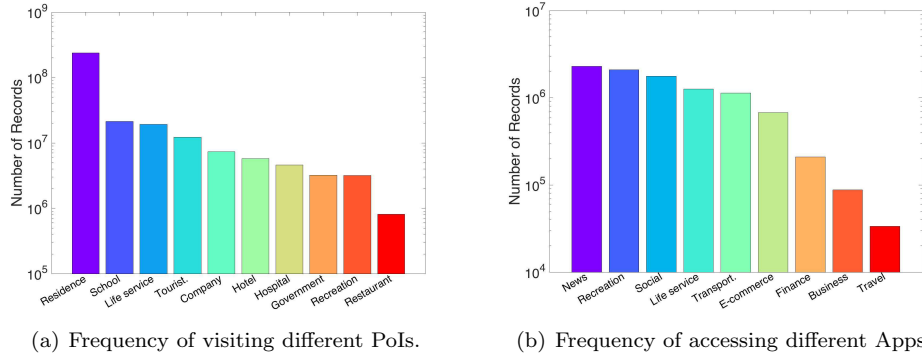


Fig. 5. The number of mobility records associated with different types of PoIs and Apps.

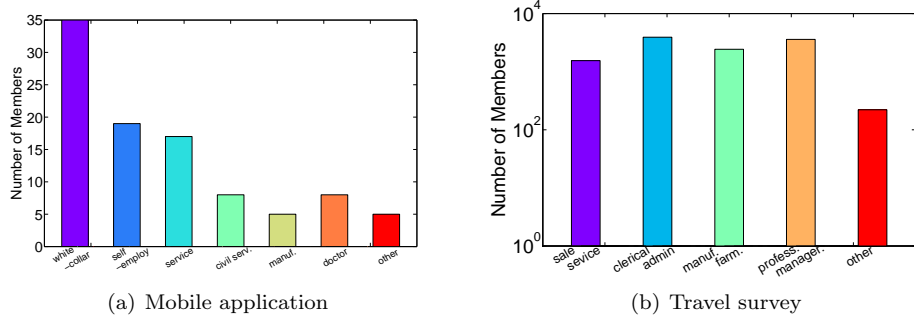


Fig. 6. The number of individuals associated with different types of occupations.

5 TEMPORAL MODES ANALYSIS ON REAL-WORLD MOBILITY DATA

5.1 Mobility Datasets

We collect three large scale real world mobility datasets to apply and evaluate our methodology. The datasets are collected from three different sources: mobile applications, cellular network and travel survey. The features of the datasets are presented in Table 1. Specifically, the details of datasets and the preprocessing procedures are discussed as follows.

Data from mobile application: This dataset is collected from the mobile devices in Beijing by a popular mobile application vendor. It records the spatiotemporal information of mobile users whenever they request localization services in the applications, such as check-in and location-based social network. The localization of the mobility records is mainly achieved by gps modules on the mobile devices plus network-based enhancement. This dataset is large scale in terms of tracing 100,000 mobile users from 17 Sep. 2016 to 31 Oct. 2016. In addition to the spatiotemporal information, this dataset provides the linkages between mobility records and *points of interest* (PoI), such as restaurants and residences. The linkages are derived from the check-ins and the spatial coverage information of PoI, which provides insights about the popular temporal modes we detect. There are 10 types of PoIs in total: residence, school, life service, tourist attraction, company, hotel, hospital, government, recreation and restaurant. The frequency of mobile users visiting different types of PoIs is presented in Figure 5(a). To explore the correlation between temporal modes and social economic status, we further collect the self-reported occupation of 103 volunteers in the data set. The distribution of different types of occupations is shown in Figure 6(a).

Data from cellular network: This dataset is collected by a major cellular network operator in Shanghai, China. It is a large scale mobility dataset also covering 100,000 mobile users with the duration of one week, between April 1st and 7th, 2016. It records the spatiotemporal information of mobile subscribers when they access cellular network (i.e., making phone calls, sending texts, or consuming data plan). Thus, the recorded locations are at the granularity of cellular base stations. Besides spatiotemporal information, it also contains the mobile applications (App) the mobile users are currently using, by resolving the *URI* of *HTTP requests*. Such associations also provide insights about understanding the popular temporal modes from another angle. There are 9 types of Apps in our dataset: news, recreation, social, life service, transportation, e-commerce, finance, business and travel. The frequency of mobile users accessing different Apps is presented in Figure 5(b).

Data from travel survey: This dataset is collected from the National Household Travel Survey(NHTS) [29] conducted from March, 2008 to March, 2009 in USA. It records the self-reported one-day transition logs of 11,712 individuals. In addition to the mobility information, it also provides the occupation information of individuals. There are 5 types occupations in this dataset, including: sales/service, clerical/admin support, manufacturer/construct/maintenance/farming workers, professional/managerial/technical and others. The distribution of occupations types in this dataset is shown in Figure 6(b). It worth pointing out that this dataset does not directly provide the spatiotemporal information of individual since the provided location is a self-reported label, such as home and office. However, we can still derive the temporal mode by partitioning the time period based on the transition records.

Privacy and ethical concerns: We have taken the following procedures to address the privacy and ethical concerns of dealing with such sensitive data. First, all of the researchers have been authorized by the application vendor and cellular network operator to utilize these two datasets for research purposes, and are bounded by strict non disclosure agreements. Second, the data is completely anonymized by replacing the users' identifiers with random sequence. Third, we store all the data in a secure off-line server, and only the core researchers can access the data.

Preprocessing: In addition to regular temporal modes, mobile users' trajectories also include spontaneous movements. To reduce the interference of spontaneous movements, we take several preprocessing procedures to derive the regular movements of typical working day and typical non-working day for each mobile user, where the non-working days includes the holidays and weekends while the working days includes the other days. Specifically, we aggregate each mobile user's mobility records into one typical working days and one typical non-working days, respectively. Then, we extract the regular movements of a mobile user by segmenting her typical days into 30-minutes time slices and associate each time slice

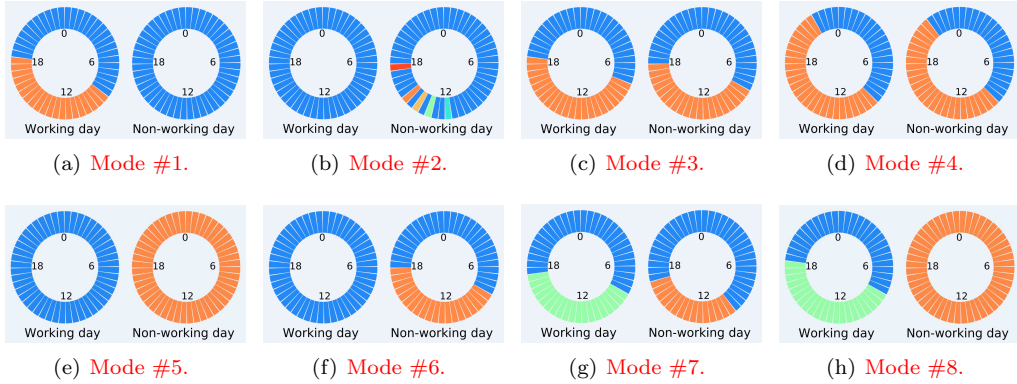


Fig. 7. The visualization of popular temporal modes detected in Beijing.

with the most frequent locations she visits in that time slice. As a result, for each mobile user we derive 48 time slices for working day and 48 time slices for non-working day, where each time slice captures the regular location she visits in that period. It worth pointing out that we filter out the mobile users with empty time slices. Thanks to the dense mobility records and long tracing period, the number of filtered out users is neglectable. **The preprocessing procedure is only applied on the mobile application and cellular network datasets, since the travel survey data only provide one day mobility information of each individual.**

5.2 The Spatiotemporal Features of Detected Popular Temporal Modes

5.2.1 Visualizing the Popular Temporal Modes. Since the travel survey dataset does not provide the concrete spatial coordinate of individuals, we first apply the proposed system on the mobile application and cellular network datasets to evaluate spatiotemporal features of popular temporal modes. As a result, we detect we detect eight popular temporal modes for Beijing and Shanghai, respectively. In order to visualize the most popular temporal modes, we present the representations of temporal modes in the form of clock dial. Specifically, there are two clock dials for each temporal mode, which stand for the 24 hours of typical working day and typical non-working day, respectively. The clock dials are segmented into 48 slices with each slices covering a 30 minutes time period, where the time slices with same colors means the mobile users stay in same locations while different colors mean otherwise. The detected popular temporal modes in Beijing and Shanghai are presented in Figure 7 and Figure 8, while the number of mobile users in each type of temporal modes is presented in Figure 9. From the results, we can observe that the popular temporal modes possess distinct characteristics and are consistent with our common intuition, since all of them exhibit a clear sleeping schedule. In addition, despite that the two datasets are collected from two different cities through two different methods, we find out the most popular 6 temporal modes are similar. It implicates that the popular temporal modes in different cities are consistent, and the proposed system are robust to different data sources. We summarize main features of these temporal modes as follow.

Mode #1: As shown in Figure 7(a) and 8(a), The most popular temporal mode in both Beijing and Shanghai exhibit similar behavior patterns. The users of this temporal mode usually go out at about 8:00 and go back at about 18:00 during working day, and stay in the same place for the whole day during non-working day. This temporal mode is consistent with the regular working schedule of a urban citizen,

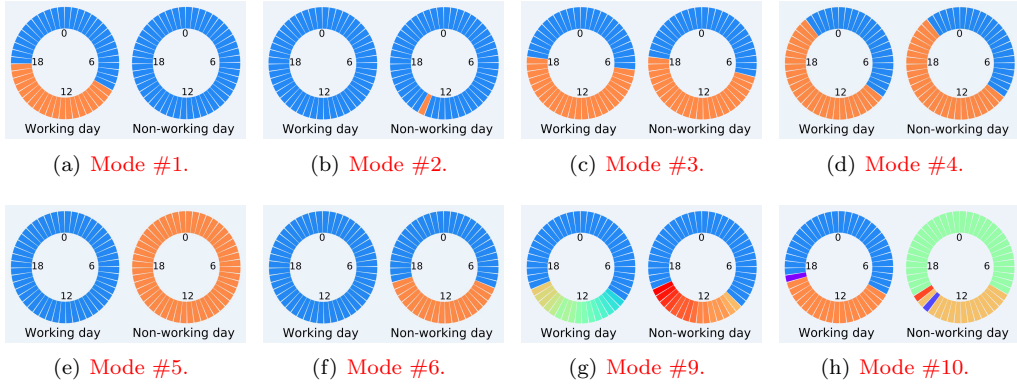


Fig. 8. The visualization of popular temporal modes detected in Shanghai.

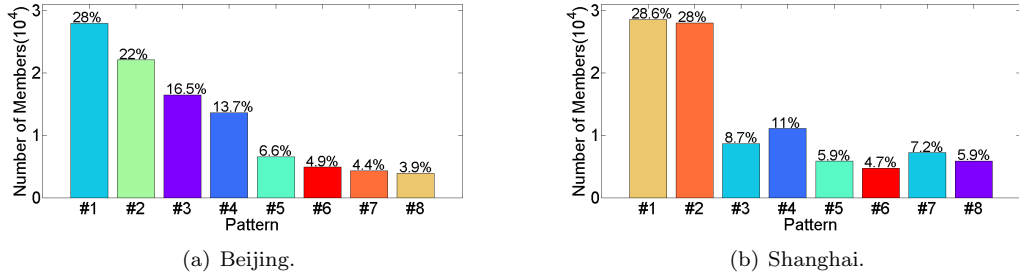


Fig. 9. The number of mobile users for each temporal mode in two cities.

and it is the most popular temporal mode which accounts for more than a quarter of total mobile users in both cities. **Mode #2:** The temporal mode #2 in both Beijing and Shanghai are also similar, which are shown in Figure 7(b) and 8(b). The distinct feature of this temporal mode is that the mobile users seldom move during working day and non-working day. **Mode #3:** The temporal mode #3 in Beijing and Shanghai are presented in 7(c) and Figure 8(c). The individuals with this temporal mode exhibit typical working schedule in both working and non-working day. **Mode #4:** The temporal mode #4 in Shanghai and Beijing are shown in Figure 7(d) and 8(d). The distinct feature is that individuals exhibit this temporal mode seem to have a long working hour, which is from about 9:00 to 21:30 for both working day and non-working day. **Mode #5:** As shown in Figure 7(e) and 8(e), the feature of temporal mode #5 is staying in one location during working day and another location during non-working day. **Mode #6:** Temporal mode #6 is presented in Figure 7(f) and 8(f). The population with this temporal mode exhibit typical working schedule during weekend. **Mode #7:** Temporal mode #7 is presented in Figure 7(g). It depicts individuals who stay in different locations during the daytime of working day and non-working day. **Mode #8:** As shown in Figure 7(h), temporal mode #8 exhibit unique temporal features that having a regular working schedule during working day, while stay in another locations during the non-working day. **Mode #9:** The #9 temporal mode is discovered in Shanghai data set, which is presented in Figure 8(g). The feature of this temporal mode is that the users stay in one location during nighttime while constantly

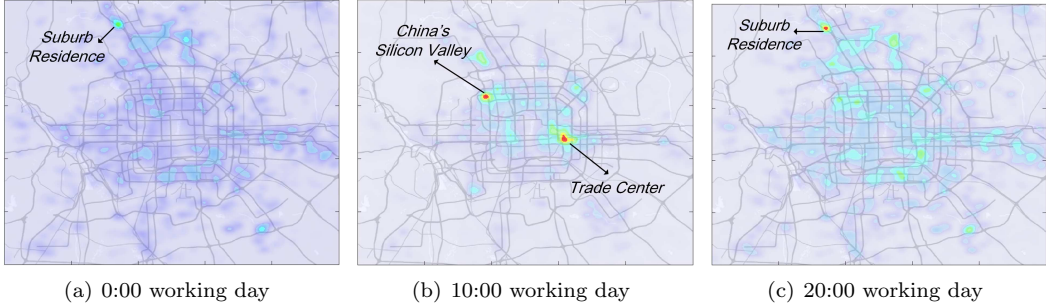


Fig. 10. Spatial distribution in working day for temporal mode #1 in *Beijing*, where population density increases gradually when color changes from blue to green to red

change their locations during daytime in both working day and non-working day. This temporal mode probably lead by taxi drivers and patrolling polices. It worth noting that the reason of this temporal mode does not occur in *Beijing* is probably because the drivers seldom activate mobile Apps in the same time of driving. **Mode #10:** The #10 temporal mode is shown in Figure 8(h). The users of this temporal mode stay in different locations during the nighttime of working day and non-working day, and their regular daytime locations of working day and non-working day are also different.

Conclusion: We detect 8 popular temporal modes in *Beijing* and *Shanghai*, respectively. We find out that there are 6 common popular temporal modes shared by *Beijing* and *Shanghai*, which indicates that the popular temporal modes in different metropolitans are consistent. However, there are also two distinct temporal modes for each city, which probably captures the differences of the citizens' daily life in these two cities.

5.2.2 Spatial Distribution of Different Temporal Modes. In our system, the extracted representations for each user's temporal mode are decoupled from location information. Since we have the spatial information in our original datasets, analyzing the spatial distribution of different temporal modes is possible, which will also lead to a deeper understanding of the detected temporal modes. Thus, we visualize the population spatial distribution of different temporal modes for both data sets in *Beijing* and *Shanghai*. Specifically, we mainly choose the time of 0:00, 10:00, 20:00 considering they are the most representative time for sleeping, working and entertaining. We visualize the spatial distribution of all the popular temporal modes, and take some typical examples for detailed discussions as follow.

Spatial Distribution in Beijing For *Beijing* city, we first look at the spatial distribution of the most popular temporal mode #1, showing in Figure 10. From the visualization, we can observe that in working day people first move to the city center (from (a) to (b)) in the morning, and then scatter to the suburbs (from (b) to (c)) in evening. In Figure 10(b), the population density in *Zhongguancun*, known as *China's Silicon Valley*, and *Guomao*, a famous *Trade Center* in *Beijing*, is significantly higher than other places. Since lots of IT companies, banks and CBDs are distributed in these two areas, it implicates that temporal mode #1 is mainly adopted by IT Engineers, civil servants and white collars work in these places.

Then, we show the spatial distribution of temporal mode #2 in Figure 11. People with this temporal mode is less active in mobility with almost unchanged spatial distribution at 0:00, 10:00 and 20:00 in working day. From Figure 11(b), we can observe that the population mainly distributed around residential

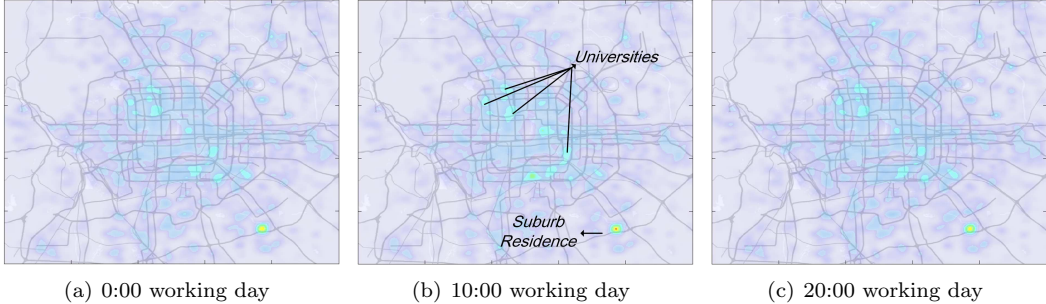


Fig. 11. Spatial distribution in working day for temporal mode #2 in *Beijing*, where population density increases gradually when color changes from blue to green to red

area and universities. Therefore, it indicates this temporal mode is possibly lead by housewives or college students.

After analyzing two typical temporal modes, we turn to compare the distributions of different temporal modes at the same time. In order to reveal the difference of working places of different temporal mode, we show the population distribution of several temporal modes at 10:00 in Figure 12. In Figure 12(a), we find out that the individuals with temporal mode #1 mainly distributed around *China's Silicon Valley* and *Trade Center* in working hours. In Figure 12(b) for temporal mode #3, people who work from 8:00 to 18:00 everyday are most likely to be concentrated in the area of *Export and Import Trade center*. In Figure 12(c), people who work from 9:00 to 22:00 both in working day and non-working day are more concentrated in *China's Silicon Valley*, which implicates IT engineers usually have a later and longer working time. In Figure 12(d) for temporal mode #5, there is a high population density in area of hospitals and primary and middle schools. Combining with the temporal features, it implicates that people may work and live in school and hospital during working day, while go back to their home in non-working day. As shown in Figure 12(e), people in temporal mode #7 mostly work in the *Trade Center*. In Figure 12(f), people with temporal mode #8 have similar distribution with temporal mode #1 in the working day, while at different location during the non-working day, which implicates that they may have weekend residence.

Spatial Distribution in Shanghai For *Shanghai* city, we first look at the spatial distribution of the most popular temporal mode #1, showing in Figure 13. Similar phenomena of daily commute can be observed in working day. Population density in *Lujiazui*, famous for its financial companies, is significantly higher than other places.

In order to show *Shanghai*'s the most intensive places for work, we compare distribution of some working-patterns at 10:00 in Figure 14. From (a) to (c), we can observe that people in temporal mode #4, #5, #10 all concentrate on the three places: *Lujiazui*, *People's Square* and *Hongqiao*. A group of famous enterprises and brands have settled in *Hongqiao* recent years and thus people with different occupations work here.

Last but not least, we visualize the spatial distribution of temporal mode #9 in Figure 15 ,which is possibly corresponding to the lifestyles of taxis driver. From (a) to (c), we can clearly observe that the population density shift from suburb areas to the city center from 8:00 to 10:00, during the morning rush hour. In addition, the population density distribute more evenly across the city center after the morning rush hours, and only part of population go back to suburbs after 18:00.

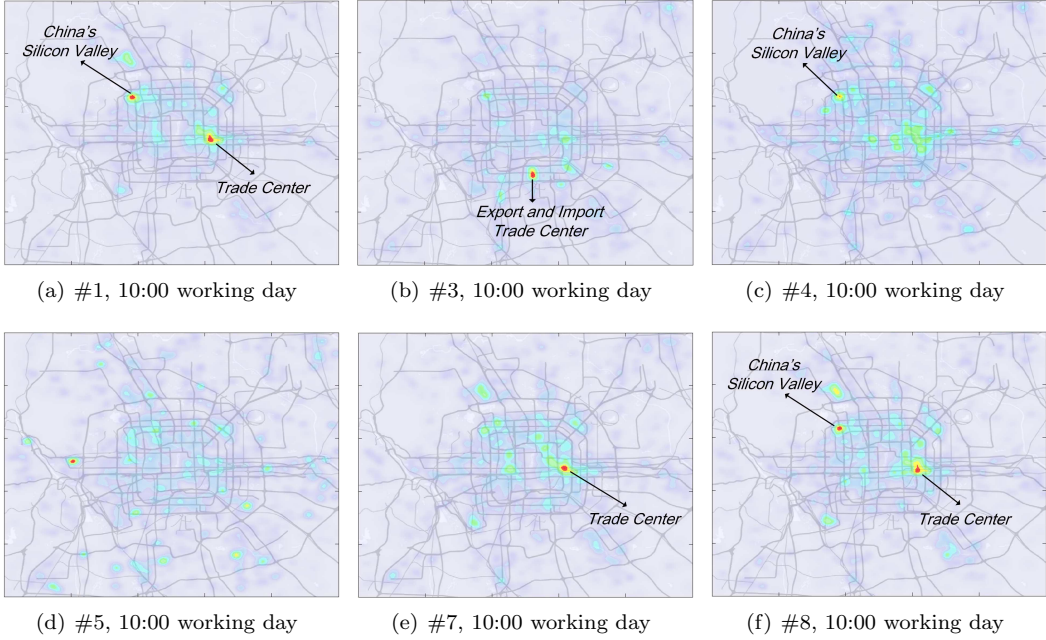


Fig. 12. Spatial distribution at 10:00 in working day for different temporal modes in *Beijing*, where population density increases gradually when color changes from blue to green to red

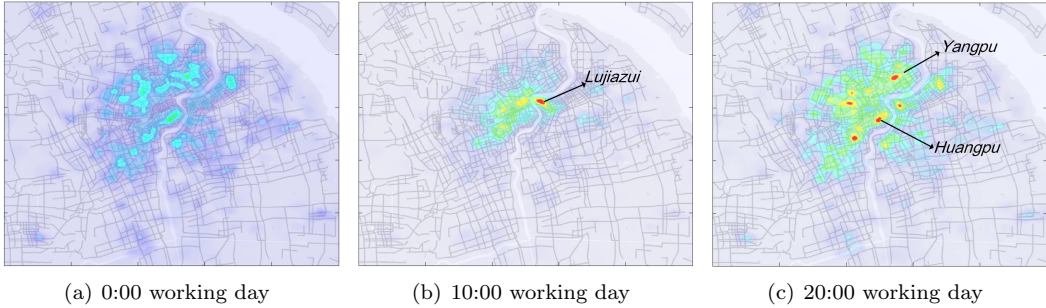


Fig. 13. Spatial distribution in working day for temporal mode #1 in *Shanghai*, where population density increases gradually when color changes from blue to green to red

5.2.3 Visualizing the Low Dimensional Projection of Temporal Modes. In the above analysis, we mainly focus on visualizing and reasoning the spatiotemporal features of popular temporal modes, which are the medoids of the detected clusters of temporal modes. In order to have a better understanding in the distribution of population's temporal modes, we utilize a high-dimensional data visualization technique[30] to project and visualize the distribution of temporal modes in 2-dimensional space. Specifically, the algorithm first builds a k-nearest neighbor graph by measuring the *partition distance* between temporal modes, and then map the graph into a 2-dimensional plane by minimizing the distortion of closeness

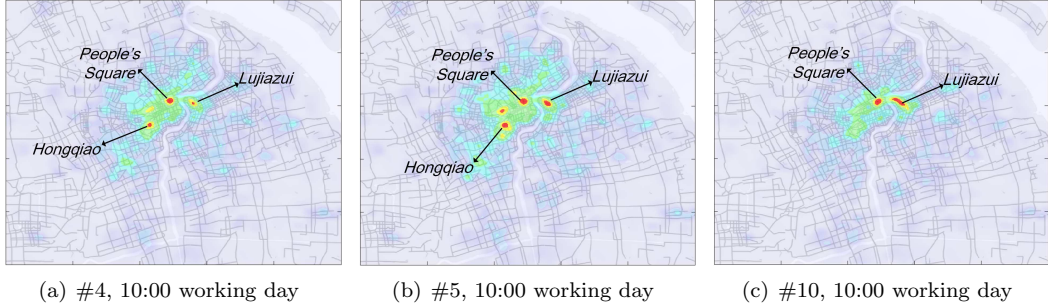


Fig. 14. Spatial distribution at 10:00 in working day for different temporal modes in *Shanghai*, where population density increases gradually when color changes from blue to green to red

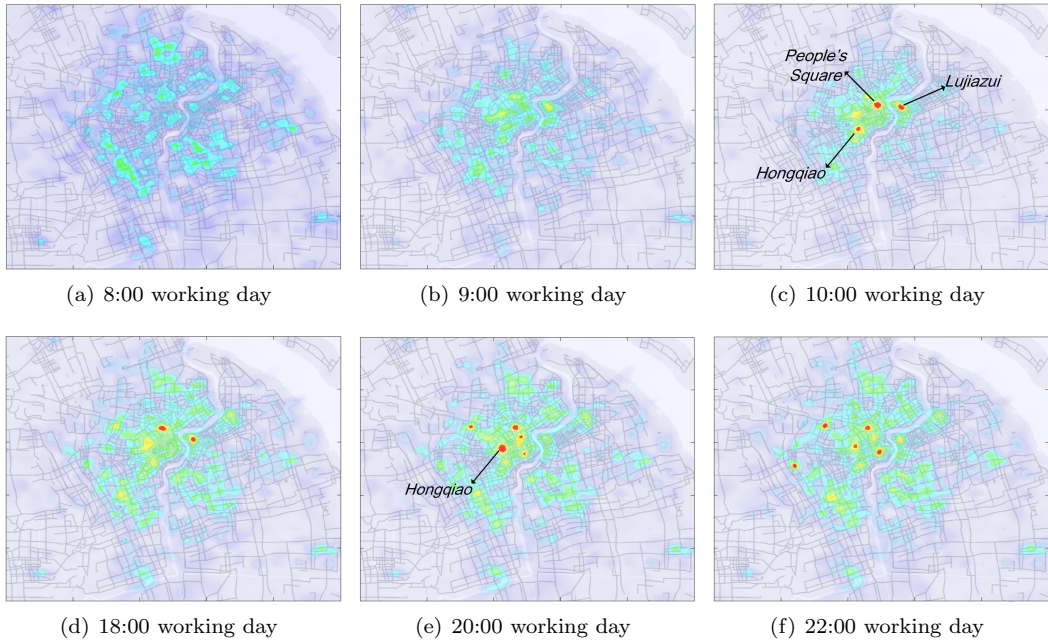


Fig. 15. Spatial distribution at different time in working day for temporal mode #9 in *Shanghai*, where population density increases gradually when color changes from blue to green to red

relation in the graph. Such mapping is designed to preserve the closeness in high-dimensional space as much as possible. The distribution of temporal modes in Beijing and Shanghai are demonstrated in Figure 16, where each point stands for the temporal mode of a user and the points with same colors represent the users with the same temporal modes.

From the results, we can explicitly observe that the users of the same popular temporal modes distribute closely to each other, while the users of different popular temporal modes generally have a larger distance. It indicates that the users within the same clusters are indeed have similar temporal

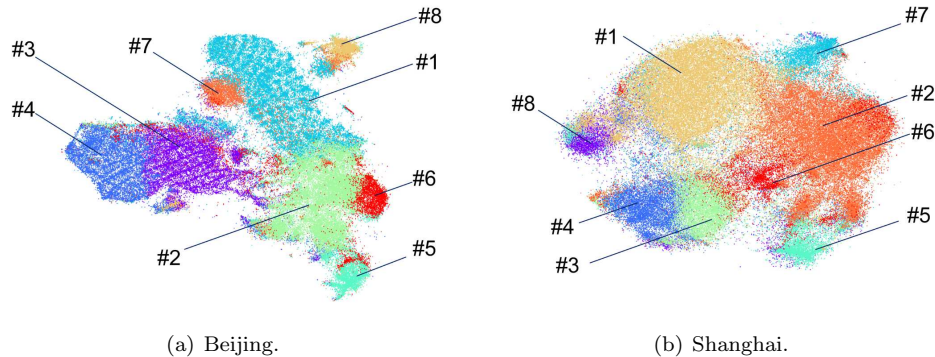


Fig. 16. Visualizing the low dimensional projection of temporal modes in two cities.

modes, and their temporal modes are close to the representative of each popular temporal mode. Therefore, the representative of each cluster is effective to represent the users within that cluster.

5.3 Revealing the Underlying Mechanism Behind Temporal Modes

In order to shed light on the underlying mechanisms behind the popular temporal modes, we aim to explore the correlations between the identified temporal modes and users' attributes, including behavior patterns and social economic status. People with different temporal modes are likely to have different social economic status, i.e., occupation, and exhibit different behaviour patterns, such as visiting PoIs and accessing Apps, in their daily life. For example, the users who have a nine to five working schedule in working day are likely to be white collars and have higher frequency in visiting the PoI of government and companies during working hours. Therefore, revealing the correlation between popular temporal modes and users' attributes is able to help us better understand the context of each temporal mode. Based on this intuition, we carry out experiments to examine how do the mobile users of different temporal modes deviate in the behaviour patterns and occupation distribution from the general population.

5.3.1 The Correlation Between Temporal Modes and User Behaviors. To achieve meaningful and truthful behavioural differences, we conduct rigorous statistical hypothesis testing on the behaviour logs of mobile users. In order to statistically prove a group of mobile users have significantly different frequency in visiting a type of PoIs than the general population, we first count the visiting frequency of each user within the group as a vector X_{group} and the visiting frequency of the whole population as a vector X_{all} . Then, we perform Student's t-test [31] on these two vectors, X_{group} and X_{all} , to examine the truthfulness of the following hypotheses:

$$\begin{aligned} H_0: \overline{X_{group}} &= \overline{X_{all}}; \\ H_1: \overline{X_{group}} &\neq \overline{X_{all}}. \end{aligned}$$

where the H_0 is the null hypothesis which indicates the average visiting frequency of the testing group does not have significant differences with general population, and H_1 is alternate hypothesis argues otherwise. The results of Student's t-test are measured by *p-value*, where the smaller *p-value* indicates higher significance level in rejecting the null hypothesis H_0 . To put it another way, smaller *p-value* indicates higher confidence in accepting the alternate hypothesis H_1 , which argues the behaviour of the

Mode	Time Slot	Restaurant	Company	Life Serv.	Tourist.	Govern.	School	Resid.	Hotel	Hospital	Recreation
#1	W: 18:30-8:30 N: 0:00-24:00	2.04	0.84	0.78**	0.76**	1.16	1.12	2.43**	0.88	0.75	0.89
	W: 8:30-18:30	1.50	2.52**	1.94**	1.64*	2.84**	0.73**	2.10**	1.53*	1.21	0.96
#2	W: 0:00-24:00 N: 18:00-11:30	0.60**	0.36**	0.50**	0.65**	1.08	1.32**	0.73**	0.71**	0.82	0.59**
	N: 11:30-18:00	0.72*	0.44**	0.62**	0.93	1.00	1.15	0.67**	0.88	0.90	0.78*
#3	W: 18:30-7:30 N: 18:00-8:00	0.32**	0.94	0.82*	0.60**	0.29**	0.36**	0.91	0.67*	0.43**	0.84
	W: 7:30-18:30 N: 8:00-18:00	1.09	0.93	2.81**	1.21	0.33**	0.40**	0.89*	0.84	0.65**	1.15
#4	W: 22:00-9:00 N: 21:30-9:00	1.50	0.87	1.40**	0.94	1.67	0.60**	1.21**	1.30	0.26**	1.62
	W: 9:00-22:00 N: 9:00-21:30	3.46**	0.73*	3.11**	1.12	0.58**	1.04	1.62**	2.28**	0.91	1.29
#5	W: 0:00-24:00	1.44	1.11	0.47**	0.75*	1.47	4.41**	0.90*	0.84	1.54*	1.31
	N: 0:00-24:00	0.66*	0.90	0.60**	1.02	1.21	1.71**	1.00	0.76	1.56*	0.76
#6	W: 0:00-24:00 N: 18:00-8:00	1.24	1.20	0.79**	1.15	0.87	1.93**	0.82**	0.82	1.32	1.08
	N: 8:00-18:00	1.40	1.35	1.21*	1.57**	0.96	1.31**	0.88**	1.04	1.15	1.23
#7	W: 17:30-8:00 N: 17:00-9:30	0.57**	0.78	0.66**	0.72**	0.81	0.62**	1.08	0.71**	0.83	0.70*
	W: 8:00-17:30	0.63**	1.47	0.70**	1.09	1.27	0.93	1.11**	0.99	1.00	0.80
	N: 9:30-17:30	0.82	0.99	0.95	1.28**	0.75**	0.96	1.01	1.10	1.34	1.00
#8	W: 18:30-8:00	1.90	0.95	1.20	1.58	3.20	0.68**	1.26**	1.25	1.24	0.82
	W: 8:00-18:30	2.22	1.63**	0.80**	1.42	3.71**	1.06	1.28**	1.54*	1.31*	1.02
	N: 0:00-24:00	0.93	0.80	0.92	1.63	1.11	0.56**	1.01	0.86	1.59*	0.62**

Table 2. The results of Student's t-test on the deviation of PoIs visiting behaviours in Beijing. The number is the ratio between the average visiting frequency in the group and in the population. * represents $p\text{-value} \leq 0.05$ and ** represents $p\text{-value} \leq 0.01$. Blocks with red colors are the distinct features. W in time slot represents working day and N represents non-working day.

testing group is different from the general population. Typically, $p\text{-value} \leq 0.05$ provides enough statistical evidence to prove the behaviour of testing group is significantly different. To analyse the correlation between popular temporal modes and mobile users behaviours, we conduct extensive Student's t-test to investigate whether the mobile users of different temporal modes deviate their PoI visiting and App usage behaviours from the population. It worth pointing out that we sample the most similar 2,500 users for each temporal mode to form the evaluation dataset in order to ensure the representative of the results.

We apply the Student's t-test on both PoI visiting and App usage records. Since PoI records usually have more explicit correlations with the context of mobility records, we investigate the contexts of temporal mode #1~#8 with them, and temporal mode #9~#10 with the App usage records. The evaluation results are presented in Table 2 and Table 3, where the value in the table is the ratio between the average accessing frequency in the group and in the population. A less than 1 value indicates the mobile users within that category have smaller frequency in given time period, and a higher than 1 value means otherwise. In addition, * marks the differences is significant with $p\text{-value} \leq 0.05$ and ** marks $p\text{-value} \leq 0.01$. Specifically, we elaborately discuss the features of each temporal mode as follows.

Temporal mode #1: From Table 2, we can observe that users have significant higher frequency in visiting company and government area during the daytime in the working day. In addition, they only exhibit regular working schedule during the working day. Therefore, this temporal mode is likely corresponding to the living styles of civil servants and white collars.

Mode	Time Slot	Business	Recreation	Social	E-commerce	Transportation	News	Finance	Travel	Life Service
#9	W: 16:30-8:30 N: 16:30-9:00	0.61	0.79	0.91	1.57	5.14**	0.49**	0.14**	0.44**	1.18
	W: 8:30-16:30	0.76	0.60*	1.04	1.16	5.63**	0.62	0.17**	0.33	1.00
	N: 9:00-16:30	0.71	0.93	0.97	0.84	4.15**	0.56*	0.00**	0.11**	0.92
#10	W: 17:30-8:00	1.67	0.56	0.96	0.48	0.80	0.59	0.52	3.44	0.77
	W: 8:00-17:30	1.61	0.52	1.03	0.84	0.55	0.48	1.10	1.50	0.73
	N: 16:00-8:00	1.03	0.44	1.11	1.08	0.62	0.58	0.70	0.99	0.70
	N: 8:00-16:00	1.14	0.58	1.11	0.60	0.76	0.64	0.55	1.90	0.85

Table 3. The Student's t-test results on the deviation of Apps usage behaviours in Shanghai. The number represents the ratio between the average accessing frequency in the group and in the population. *represents $p\text{-value} \leq 0.05$ and **represents $p\text{-value} \leq 0.01$. Blocks with red colors are the distinct features. W in time slot represents working day and N represents non-working day.

Temporal mode #2: The distinct feature temporal mode #2 is that the users have significantly higher frequency in visiting school, while they have significantly lower frequency stay in company and residence area. These users are likely to be boarding students who live in campus.

Temporal mode #3: We can observe that these users visit life services PoI about 3 times more frequent than general population, and the differences pass hypothesis testing with $p\text{-value} \leq 0.01$. In addition, they are less likely to be in the area of school or government area. The possible reason is that these users are service providers who stay in life services area in the daytime of both working day and non-working day, such as shop assistants.

Temporal mode #4: Users with this temporal mode are more likely to be in a restaurant, hotel and life service area during the daytime. They have the similar temporal mode of working every day as the users with temporal mode #3, but with longer working hours. Therefore, they are likely to be waiters, security guards or shop assistants who work on shift everyday.

Temporal mode #5: These users have significantly higher frequency in visiting school and hospital, while they stay in different locations for working day and non-working day. They are likely corresponding to the boarding school students or resident doctors who stay in school and hospital during the working day and return home during non-working day.

Temporal mode #6: From Table 2, we can observe that frequency of visiting tourist attractions PoI during daytime of the non-working day and stay in school for the rest of time are significantly higher than general population. Boarding students who live in campus in working day and hang out in non-working day match this kind of temporal mode.

Temporal mode #7: These users are more likely to be in tourist attractions during the daytime in non-working day. Therefore, they are likely to be the people who enjoy entertaining in tourist attractions area in non-working day. Typical social groups are people who like to travel on weekends.

Temporal mode #8: The users with temporal mode #8 are more likely to be in a company or government during the daytime in working day. They work during the daytime in working day and return home at dusk, but they move to a new place in non-working day. Typical social groups of this category are civil servants and white collars who live in a different place on non-working day.

Temporal mode #9: From Table 3, we can observe that these users are much more likely to use transportation Apps like maps and taxi apps and less likely to use finance apps. In addition, they are

Mode	Feature of temporal modes	Feature of PoIs and Apps	Potential Social Groups
#1	{W: 18:30-8:30 N: 0:00-24:00}, {W: 8:30-18:30}	company, government	civil servant, white collar
#2	W: 0:00-24:00 N: 18:00-11:30; N: 11:30-18:00	school	boarding student, housewife
#3	W: 18:30-7:30 N: 18:00-8:00; W: 7:30-18:30 N: 8:00-18:00	life service	shop assistant
#4	W: 22:00-9:00 N: 21:30-9:00; W: 9:00-22:00 N: 9:00-21:30	restaurant, hotel, life service	waiter, security guard, shop assistant
#5	W: 0:00-24:00; N: 0:00-24:00	school, hospital	boarding student, patient
#6	W: 0:00-24:00 N: 18:00-8:00; N: 8:00-18:00	school, tourist attraction	boarding student
#7	W: 17:30-8:00 N: 17:00-9:30; W: 8:00-17:30; N: 9:30-17:30	company, government	civil servant, white collar
#8	W: 18:30-8:00; W: 8:00-18:30; N: 0:00-24:00	tourist attraction	civil servant, white collar
#9	W: 16:30-8:30 N: 16:30-9:00; W: 8:30-16:30; N: 9:00-16:30	transportation apps like maps	taxis driver

Table 4. The summary of temporal mode features, behaviours features and potential social groups for each category.

constantly moving during the daytime both in working day and non-working day. Therefore, they are likely corresponding to the taxi drivers.

To conclude, the defining features of user behaviours and temporal modes as well as the potential social groups for each temporal mode are summarized in Table 4. Through the Student's t-test, we reveal the correlation between temporal modes and user behaviours, which provides deep insight about the mechanisms behind popular temporal modes.

5.3.2 The Correlation Between Temporal Modes and Social Economic Status. To explore the correlation between popular temporal modes and social economic status, we evaluate our system on the mobile application dataset and travel survey dataset with the self-reported occupations. Specifically, in mobile application dataset we have 103 samples, and in travel survey dataset we have 11,712 samples, where both occupation information and temporal modes can be derived.

As for the mobile application dataset, we present the confusion matrix between popular temporal modes and occupations in Table 5. Since there are different number of individuals within each temporal mode, we normalized the confusion matrix with the number of individuals within each temporal mode. For example, the first entry in the table — 0.781 indicates about 78% of individuals with temporal mode #1 have the occupation of white collar. To illustrate the main features of the matrix, we highlight the maximum value of each column with red color. We find out that the confusion matrix reveals a strong correlation between popular temporal modes and occupations. Specifically, the individuals exhibit typical working schedule in working day, i.e., temporal mode #1, #7 and #8, are significantly more likely to have occupations in white collar and civil servant category. In addition, the individuals that have long working hours or have working schedule in non-working day, i.e., temporal mode #3, #4 and #6, tend to have occupations in service category. Finally, the individuals with low mobility, i.e., temporal mode #2, are more likely to have occupations in self-employed category.

As for the travel survey dataset, we first extract the temporal modes of individuals as how they partition a typical working day, since the dataset only provides the transition records of each individual for one working day. Then, we apply our system to detect the popular temporal modes among the population, which are visualized in Figure 17. From the figures, we observe that there are five distinct popular temporal modes in travel survey dataset. Specifically, temporal mode #14 and #15 exhibit nine to five working schedule and low mobility in working day, which are similar with working day behaviors in temporal mode #1 and #2, respectively. In addition, temporal mode #13 exhibits distinct feature as an earlier working schedule, while #12 visits another location at the end of working hour. Since this dataset

Occupation \ Mode	#1	#2	#3	#4	#5	#6	#7	#8
white collar	0.781	0.185	0.000	0.062	0.000	0.200	0.000	0.600
self-employed	0.000	0.481	0.111	0.250	0.000	0.000	0.167	0.000
service	0.000	0.074	0.555	0.313	0.333	0.400	0.167	0.200
others	0.000	0.037	0.000	0.062	0.333	0.200	0.167	0.000
civil servant	0.156	0.037	0.111	0.125	0.333	0.200	0.333	0.200
manufacturing	0.000	0.111	0.111	0.062	0.000	0.000	0.000	0.000
doctor	0.062	0.074	0.111	0.125	0.000	0.000	0.167	0.000

Table 5. Normalized confusion matrix of popular temporal modes and occupations in mobile application dataset, where the value is normalized by the number of individuals with each temporal mode and the maximum value of each column is highlighted.

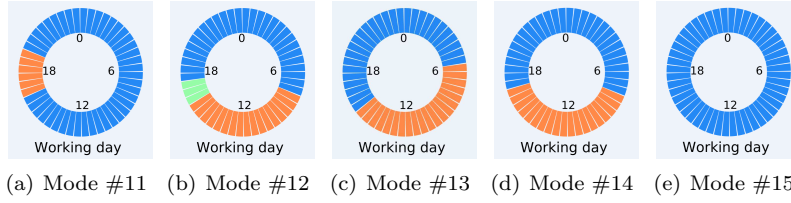


Fig. 17. The visualization of popular temporal modes detected in travel survey dataset.

is collected in USA in 2008, we can observe that two temporal modes(i.e., #14 and #15) are consistent with our findings in other two datasets, while the other three temporal modes have distinct features.

After visualizing the features of popular temporal modes, we present the confusion matrix between temporal modes and occupations in Table 6, where the value is also normalized by the number of individuals in each temporal mode and the maximum value of each column is highlighted. The confusion matrix demonstrates a strong correlation between popular temporal modes and occupations. About 82% of individuals with temporal mode #15 and 94% temporal mode #11 have the occupations in sales and service category. These two temporal modes exhibit low mobility during working day that only occasionally visit another location in afternoon, which is likely corresponding to shop assistances who live in store or have a self-own business. In addition, the individuals with nine to five working schedule as temporal mode #14 tend to occupations in professional, managerial and technical category, while those visit another locations at the end of working hours as temporal mode #12 tend to have occupations in clerical and admin support category. Finally, the individuals with an earlier working schedule as temporal mode #13 are more likely to have occupations in manufacturing, constructing, maintenance and farming category.

To conclude, the experiments demonstrate that the detected popular temporal modes indeed have a strong correlation with user behavior patterns and social economic status, where the individuals with same temporal modes tend to have similar behavior patterns and occupations and the individuals of different temporal modes have distinct features. The experiment results are consistent with previous spatiotemporal visualization and our assumptions on mechanisms behind popular temporal modes. These

Occupation \ Mode	#11	#12	#13	#14	#15
sale,sevice	0.939	0.000	0.000	0.000	0.821
clerical,admin support	0.000	0.520	0.173	0.456	0.014
manuf.,const.,mainten.,farm.	0.000	0.076	0.793	0.067	0.024
profess.,manager.,technical	0.005	0.404	0.034	0.477	0.000
other occupations	0.056	0.000	0.000	0.000	0.141

Table 6. Normalized confusion matrix of popular temporal modes and occupations in travel survey dataset, where the value is normalized by the number of individuals with each temporal mode and the maximum value of each column is highlighted.

findings not only deepen our understanding on urban mobility, but also demonstrate the potential on leveraging the features of temporal modes in user behavior profiling and social economic status inferring.

5.4 Performance Gain Comparing with Baseline Method

To further evaluate the effectiveness of our system, we implement a state-of-art trajectory clustering algorithm as baseline, which first extract latent features from raw trajectory data with *latent dirichlet allocation*(LDA) algorithm[32] and then cluster the trajectories based on the latent features. The baseline is a widely adopted algorithm in trajectory data mining [5, 14]. The LDA algorithm is originally designed to extract latent semantic feature for words and documents based on their co-occurrences frequency. Specifically, the baseline treats the mobility records as words and trajectories as documents, and extract latent features for both mobility records and trajectories with LDA algorithm. Then, it utilizes kmeans algorithm to detect the clusters of mobility records and trajectories in latent feature space, respectively. We aim to compare our system with the baseline in terms of the performance in detecting semantic-rich clusters of trajectories and mobility records, which is evaluated as correlation with occupations and user behaviors. Therefore, we evaluate our system and baseline algorithm on mobile application dataset, because it contains the information of both occupation and POI visitation. Since we detect 8 popular temporal modes and 18 temporal mode feaures on mobile application dataset(shown in Table 4), we considered the trajectory with same popular temporal modes as the trajectory clusters and mobility records within the same temporal mode features(e.g. 8:30~18:30 in working day for temporal mode #1) as mobility records clusters that identified by our system. To compare with our system, we set number of latent feature as 18, number of trajectory cluster as 8 and number of mobility records cluster as 18 in baseline algorithm.

To quantitatively evaluate the performance gain of our system, we utilize a information theory based metric — normalized mutual information(NMI), which is a widely adopted performance metric in clustering analysis[33]. Denote Y_k as the set of mobility records(trajactories) associate with the k -th type PoIs(occupations), Z_j as set of mobility records(trajactories) that are classified into the j -th cluster and M as the total number of mobility records(trajactories). The NMI can be computed as follow,

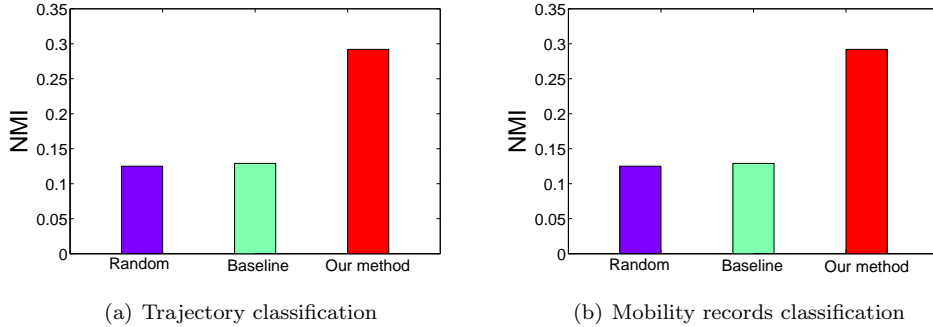


Fig. 18. Performance differences between random assignment, baseline algorithm and our system in classifying trajectories into different occupations and mobility records into PoI visitations.

$$\begin{aligned}
 I(Y, Z) &= \sum_k \sum_j \frac{|Y_k \cap Z_j|}{M} \log_2 \frac{M|Y_k \cap Z_j|}{|Y_k||Z_j|}, \\
 H(\star) &= - \sum_{\forall X_i \in \star} \frac{|X_i|}{\sum_{\forall X_i \in \star} |X_i|} \log \left(\frac{|X_i|}{\sum_{\forall X_i \in \star} |X_i|} \right), \\
 NMI(Y, Z) &= \frac{2 \times I(Y, Z)}{H(Y) + H(Z)},
 \end{aligned} \tag{1}$$

where $H(\star)$ is the entropy of mobility records(trajectories), and $I(Y, Z)$ quantifies the mutual information between the PoIs(occupations) categories and the identified mobility records(trajectories) clusters. Therefore, $NMI(Y, Z)$ is the normalized mutual information, which is bounded between 0 and 1. If NMI reaches to 1, it indicates the cluster result obtain all information of PoI(occupations) types, i.e, all the mobility records(trajectories) associated with same PoI(occupation) types are correctly classified into same clusters. We present the performance differences between random assignment, baseline algorithm and our system in classifying trajectories into different occupations and mobility records into PoI visitation in Figure 18. Figure 18(a) demonstrates that our system significantly outperforms the random assignment and baseline method in trajectory classification task in terms of achieving 126.4% performance improvement in NMI. From Figure 18(b), we observe that our system also achieves 112.5% performance gain in mobility records classification task comparing with the baseline algorithm. These results indicates our system significantly outperforms baseline trajectory clustering algorithm in achieving semantic-rich trajectory analysis, which is classifying trajectories into occupations and mobility records into PoI visitations. In addition, we observe that baseline algorithm only has small performance gain comparing with random assignment, which is probably because it extracts latent features from trajectories based on co-occurrences frequency of mobility records and unable to capture semantic features of trajectories. We believe our system tackles an important problem in semantic analysis of large-scale unlabelled trajectory data.

6 LIMITATIONS AND FUTURE WORKS

In this section, we discussed the limitations and future works of our research.

Firstly, the occupation information in mobile application dataset is collected from 103 volunteers, which inevitably introduces sampling biases(e.g., self-selected biases). However, the experiments on travel survey dataset, which is large-scale and collected from completely different population, render consistent results with mobile application dataset on the correlation between popular temporal mode and user's occupations. These results lend confidence on the representative and generality of our findings. One of future works will be to conduct a more thorough qualitatively study on the mechanism behind temporal modes, such as interviewing the individuals with different temporal modes.

Secondly, since the popular temporal modes are detected based on the patterns of allocating time across different locations, a reasonably dense mobility dataset is required to detect reliable temporal modes. Although our system has introduced techniques to handle the data sparsity in spatial and temporal domain, it still cannot reliably produce high quality temporal modes when data sparsity is high, e.g, check-in records. Therefore, one open future work is to extend current system to highly sparse mobility data.

7 CONCLUSION

In this paper, we investigate the problem of detecting popular temporal modes embedded in large scale unlabelled mobility data. Toward this end, we propose a pipeline system that sequentially addresses the problems of: 1) eliminating the noises in localization; 2) extracting representations for temporal modes; and 3) identifying popular temporal modes. The evaluations on three real-world mobility dataset demonstrate that our system can effectively detect the popular temporal modes, which are easy to be interpreted and exhibit meaningful characteristics. In addition, our further investigation reveals that mobile users' behaviours(e.g. accessing mobile Apps and visiting PoIs) and social economic status(i.e., occupations) are closely correlated with the identified temporal modes. By leveraging these correlations, our system manages to significantly outperform baseline algorithm by 112.5 and 126.4% in classifying mobility records into PoI visitations and trajectories into occupations, respectively. We believe that this work opens a new angle to model mobile users' behavioural patterns in large scale unlabelled mobility data, and paves the way toward understanding the underlying mechanisms behind urban mobility.

REFERENCES

- [1] Charles A Eldering. Advertisement selection system supporting discretionary target market characteristics. 2003.
- [2] Junping Zhang, Fei Yue Wang, Kunfeng Wang, Wei Hua Lin, Xin Xu, and Cheng Chen. Data-driven intelligent transportation systems: A survey. *IEEE Transactions on Intelligent Transportation Systems*, 12(4):1624–1639, 2011.
- [3] Nikola Banovic, Tofi Buzali, Fanny Chevalier, Jennifer Mankoff, and Anind K. Dey. Modeling and understanding human routine behavior. In *CHI Conference*, pages 248–260, 2016.
- [4] Jae Gil Lee, Jiawei Han, and Kyu Young Whang. Trajectory clustering:a partition-and-group framework. In *ACM SIGMOD International Conference on Management of Data*, pages 593–604, 2007.
- [5] Ke Zhang, Yu Ru Lin, and Konstantinos Pelechrinis. Eigentransitions with hypothesis testing: The anatomy of urban mobility. In *Tenth International AAAI Conference on Web and Social Media*, 2016.
- [6] Jia Ching Ying, Wang Chien Lee, Tz Chiao Weng, and Vincent S. Tseng. Semantic trajectory mining for location prediction. In *ACM Sigspatial International Conference on Advances in Geographic Information Systems*, pages 34–43, 2011.
- [7] Nathan Eagle and Alex Sandy Pentland. Eigenbehaviors: identifying structure in routine. *Behavioral Ecology and Sociobiology*, 63(7):1057–1066, 2009.
- [8] Hoyoung Jeung, Lung Yiu Man, and Christian S. Jensen. Trajectory pattern mining. In *ACM SIGKDD International Conference on Knowledge Discovery and Data Mining*, pages 330–339, 2007.
- [9] Nikos Mamoulis, Huiping Cao, George Kollios, Marios Hadjieleftheriou, Yufei Tao, and David W. Cheung. Mining, indexing, and querying historical spatiotemporal data. In *Tenth ACM SIGKDD International Conference on Knowledge Discovery and Data Mining, Seattle, Washington, USA, August*, pages 236–245, 2004.

- [10] Yu Zheng, Lizhu Zhang, Xing Xie, and Wei Ying Ma. Mining interesting locations and travel sequences from gps trajectories. In *International Conference on World Wide Web, WWW 2009, Madrid, Spain, April*, pages 791–800, 2009.
- [11] Richard Becker, Karrie Hanson, Sibren Isaacman, Meng Loh Ji, Margaret Martonosi, James Rowland, Simon Urbanek, Alexander Varshavsky, and Chris Volinsky. Human mobility characterization from cellular network data. *Communications of the Acm*, 56(1):74–82, 2013.
- [12] Sibren Isaacman, Richard Becker, Margaret Martonosi, James Rowland, Alexander Varshavsky, and Walter Willinger. Human mobility modeling at metropolitan scales. In *Proceedings of the 10th international conference on Mobile systems, applications, and services*, pages 239–252, 2012.
- [13] S. Jiang, Y. Yang, S Gupta, D Veneziano, S Athavale, and M. C. Gonzlez. The timegeo modeling framework for urban mobility without travel surveys. *Proceedings of the National Academy of Sciences of the United States of America*, 113(37):E5370, 2016.
- [14] Jing Yuan, Yu Zheng, and Xing Xie. Discovering regions of different functions in a city using human mobility and pois. In *ACM SIGKDD International Conference on Knowledge Discovery and Data Mining*, pages 186–194, 2012.
- [15] Sergej Sizov. Geofolk:latent spatial semantics in web 2.0 social media. In *International Conference on Web Search and Web Data Mining, WSDM 2010, New York, Ny, Usa, February*, pages 281–290, 2010.
- [16] Huandong Wang, Fengli Xu, Yong Li, Pengyu Zhang, and Depeng Jin. Understanding mobile traffic patterns of large scale cellular towers in urban environment. *IEEE/ACM Transactions on Networking*, PP(99):1–15, 2015.
- [17] Zipei Fan, Xuan Song, and Ryosuke Shibasaki. Cityspectrum: a non-negative tensor factorization approach. In *ACM International Joint Conference on Pervasive and Ubiquitous Computing*, pages 213–223, 2014.
- [18] Justin Cranshaw, Raz Schwartz, Jason I Hong, and Norman Sadeh. The livehoods project: Utilizing social media to understand the dynamics of a city. *Social Science Electronic Publishing*, 1977.
- [19] Matthew L Daggitt, Noulas Anastasios, Shaw Blake, and Mascolo Cecilia. Tracking urban activity growth globally with big location data. *Royal Society Open Science*, 3(4), 2015.
- [20] Chao Zhang, Keyang Zhang, Quan Yuan, Haoruo Peng, Yu Zheng, Tim Hanratty, Shaowen Wang, and Jiawei Han. Regions, periods, activities: Uncovering urban dynamics via cross-modal representation learning. In *Proceedings of the 26th International Conference on World Wide Web, WWW 2017, Perth, Australia, April 3-7, 2017*, pages 361–370, 2017.
- [21] Chaoming Song and Albert Lszl Barabsi. Limits of predictability in human mobility. *Science*, 327(5968):1018, 2010.
- [22] Ailin Mao, Christopher G. A. Harrison, and Timothy H. Dixon. Noise in gps coordinate time series. *Journal of Geophysical Research Atmospheres*, 104(B2):2797–2816, 1999.
- [23] Alex Rodriguez and Alessandro Laio. Clustering by fast search and find of density peaks. *Science*, 344(6191):1492–6, 2014.
- [24] Gusfield Dan. Partition-distance: A problem and class of perfect graphs arising in clustering. *Information Processing Letters*, 82(3):159–164, 2002.
- [25] Giovanni Rossi. Partition distances. *Computer Science*, 2011.
- [26] Dmitry A Konovalov, Bruce Litow, and Nigel Bajema. Partition-distance via the assignment problem. *Bioinformatics*, 21(10):2463–2468, 2005.
- [27] H. W Kuhn. The hungarian method for the assignment problem. *Naval Research Logistics*, 52(1):83–97, 2005.
- [28] A. K Jain, M. N Murty, and P. J Flynn. Data clustering: a review. *Acm Computing Surveys*, 31(3):264–323, 1999.
- [29] Federal Highway Administration U.S. Department of Transportation. 2009 national household travel survey. 2009.
- [30] Jian Tang, Jingzhou Liu, Ming Zhang, and Qiaozhu Mei. Visualizing large-scale and high-dimensional data. 37(7):287–297, 2016.
- [31] Student (W S Gosset. The probable error of a mean. *Biometrika*, 6(1):1–25, 1908.
- [32] David M Blei, Andrew Y Ng, and Michael I Jordan. Latent dirichlet allocation. *Journal of Machine Learning Research*, 3:993–1022, 2003.
- [33] Mo Chen. Normalized mutual information. *Information Theory*.

Received May 2017